Food Control 110 (2020) 106981

Contents lists available at ScienceDirect

Food Control

journal homepage: www.elsevier.com/locate/foodcont

Discriminating muscle type of selected game species using near infrared (NIR) spectroscopy

Pholisa Dumalisile[a], Marena Manley[a], Louwrens Hoffman[b,1], Paul J. Williams[a,*]

[a] Department of Food Science, Stellenbosch University, Private Bag X1, Matieland (Stellenbosch), 7602, South Africa
[b] Department of Animal Science, Stellenbosch University, Private Bag X1, Matieland (Stellenbosch), 7602, South Africa

ARTICLE INFO

Keywords:
Near infrared spectroscopy
Discrimination
Multivariate analysis
Muscle types
Game meat
Food fraud

ABSTRACT

In this study near infrared (NIR) spectroscopy was used to discriminate between different muscle types within each species of selected game animals, and to classify species regardless of the muscle. Muscle steaks from *longissimus thoracis et lumborum* (LTL) located at the 6th rib of the carcasses, *infraspinatus* (IS) and *supraspinatus* (SS) located on the forequarter, and *biceps femoris* (BF), *semitendinosus* (ST) and *semimembranosus* (SM) located on the hindquarter of impala and eland species; and samples from fan fillet (FF), big drum (BD), triangle steak (TS), moon steak (MS) and rump steak (RS) of ostrich species were scanned with a handheld NIR spectrophotometer in the spectral range of 908–1700 nm. Spectra were pre-treated with different pre-processing methods and classification models were developed using partial least squares discriminant analysis (PLS-DA). Classification accuracies were higher when the muscles were grouped according to their anatomical location in the carcass, than attempting to classify them separately. Classification accuracies ranging from 85.0 to 100% were achieved throughout, with forequarter muscles yielding the highest classification accuracy rate for both impala and eland species. Furthermore, when the species were discriminated regardless of muscles, PLS-DA models pre-treated with SNV-Detrend and Savitzky-Golay 1st derivative yielded accuracies of 97, 81 and 92% for eland, impala and ostrich, respectively. These results indicate that NIR spectroscopy can be used for the authentication of game meat, specifically impala, eland and ostrich. Furthermore, it was easier to discriminate species regardless of the muscle used than different muscles within each species.

1. Introduction

The deception of consumers by retailers selling substituted food products for economic gain is illegal (DoH, 2014), and in the food industry it is termed food fraud. As tempting as it may be to retailers or suppliers, the consequences of food fraud are destructive and may include damaging the company's reputation (Van Ruth, Luning, Silvis, Yang, & Huisman, 2018). Food fraud is defined by Spink and Moyer (2011) as a collective term used to encompass the deliberate and intentional substitution, addition, tampering, or misrepresentation of food, food ingredients, or food packaging; or false or misleading statements made about a product, for economic gain.

Meat and meat products are often targets of food fraud, and are currently leading the top 5 list of EU food categories of illegal import fraud examples (Soon & Manning, 2018). Finding horse meat in beef burgers produced in Ireland in 2013 showed that consumers are undoubtedly encountering undeclared animal species in meat products (O'Mahony, 2013; Walker, Burns, & Burns, 2013). In South Africa, Cawthorn, Steinman, and Hoffman (2013) found species in beef sausages that were not declared on the product labelling. Thus, the reported and unreported incidents of undeclared labelling of meat products have subsequently raised the consumers' awareness of quality, traceability and origin of the food they eat (Verbeke & Ward, 2006).

Consumers are very aware of the different muscle types (cuts) and their retail value, mainly due to quality differences. When a customer decides which meat species to buy, the next decision is to choose the

* Corresponding author.
E-mail address: pauljw@sun.ac.za (P.J. Williams).
[1] Current address: Centre for Nutrition and Food Sciences, Queensland Alliance for Agriculture and Food Innovation, The University of Queensland, Coopers Plains, QLD 4108, Australia.

https://doi.org/10.1016/j.foodcont.2019.106981
Received 17 July 2019; Received in revised form 25 October 2019; Accepted 1 November 2019
Available online 02 November 2019
0956-7135/

muscle type. In most cases tenderness and selling price tend to influence this decision. It is then disappointing and fraudulent to purchase what is thought to be a tender expensive muscle, only to discover it is tough and likely a low-priced muscle. Thus, mislabelling of food products is a serious issue that can even potentially affect the country of origin, in the case of exported products. Proper labelling of meat products is important to help fair trade and to enable consumers to make informed choices (DoA, 2015; DoH, 2014). In South Africa, there are regulatory bodies governing food legislation. The Foodstuff, Cosmetics and Disinfectant Act, under the Department of Health (DoH), controls the labelling and advertising guidelines of meat and meat products to ensure consumers are not misled and given false information (DoH, 2014). As much as there are regulations in place to protect consumers, the food products need to be verified (authenticated). Food authentication is a procedure that verifies that food complies with its label description (Danezis, Tsagkaris, Camin, Brusic, & Georgiou, 2016).

Authenticity issues associated with substitution of meat and its products are identified by a variety of standard analytical methods (chromatography, electrophoretic separation of proteins, enzyme-linked immunosorbent assay (ELISA) procedures and DNA based techniques) available (Cawthorn et al., 2013; Fajardo, González Isabel, Rojas, García, & Martín, 2010; Jonker, Tilburg, Hagele, & de Boer, 2008; Nakyinsige, Man, & Sazili, 2012). However, all of these are tedious, costly, require complicated laboratory procedures and hazardous solvents, need skilled personnel and sample preparation, with most of them also including a destructive step that damages or lowers the quality of the product being tested (Kamruzzaman, Sun, ElMasry, & Allen, 2013; Manley, 2014). Therefore, there is a need of a rapid, chemical-free method and near infrared (NIR) spectroscopy offers this.

Kamruzzaman, Elmasry, Sun, and Allen (2011) used NIR hyperspectral imaging to discriminate lamb muscles (*Semitendinosus* (ST), *Longissimus dorsi* (LD) and *Psoas major* (PM)) in a wavelength range of 900–1700 nm. They used principal component analysis (PCA) for wavelength reduction and linear discriminant analysis (LDA) (Fisher, 1936) to build classification models. The results showed that it was possible to discriminate between the three lamb muscles with an overall accuracy of 100%. Similarly, Sanz et al. (2016) discriminated lamb muscles using hyperspectral imaging in the wavelength range of 380–1028 nm, in a follow-up to the conclusions of Kamruzzaman et al. (2011) by including an additional muscle type and using more samples. In their work, they used four different muscle types (LD, ST, PM and *Semimembanosus* (SM)) from 30 animals of a different breed to that Kamruzzaman et al. (2011) used and found that the Linear Least Mean Squares (LMS) classifier gave the best classification accuracy of 96.67%. They also found that the inclusion of an additional muscle (SM) made the classification problem more complex. Furthermore, Alomar, Gallo, Castañeda, and Fuchslocher (2003) segregated different types of bovine meat and predicted several chemical fractions from two breeds and three muscles (LD, ST and *Supraspinatus* (SS)) using NIR spectroscopy in a wavelength range of 400–2500 nm. The results showed the two breeds were correctly classified with 78.8% accuracy and the three muscle types yielded 97.8 (LD), 97.7 (SS) and 89.5% (ST) classification accuacy.

Game meat offers a healthy alternative to red meat consumers, as it contains low fat and high protein levels (Hoffman, 2007). It is known that within an animal, different muscles have diverse textural and chemical properties (Van Ba, Park, Dashmaa, & Hwang, 2014). Moreover, different muscle types differ in their retail price as their quality is not the same, for example fillet is more expensive than sirloin steak. To date, no study has been done on rapid techniques to support the authenticity of different muscle types within species of South African game meat. Therefore, the aim of this study was to investigate the ability of NIR spectroscopy in discriminating selected game muscle types and, to discriminate different species irrespective of the muscle used.

Table 1
The total number (females and males) of impala, eland and ostrich species and their average weight (kg).

Species	Total number	Sex		Average Weight (kg)
		Females	Males	
Impala	12	0	12	37.1
Eland	15	7	8	337.3
Ostrich	15	4	11	85.9

2. Material and methods

2.1. Meat samples

Meat samples were obtained from carcasses of three different game species. A total of 42 animals from the following species were harvested from farms in Bredasdorp and Oudtshoorn, South Africa: 12 Impala (*Aepyceros melampus*), 15 Eland (*Taurotragus oryx*) and 15 Ostrich (*Struthio camelus*). All of these species were harvested in winter. The ostriches were semi-domesticated hence their age could be determined (10 months old), whereas eland and impala were free roaming feeding/grazing on natural vegetation hence their age could not be determined at the time of slaughter. The sex of all animals was known and is illustrated in Table 1. All animals were harvested according to the standard operating procedure (Van Schalkwyk & Hoffman, 2010) with ethical clearance (approval number: SU-ACUM14-001SOP; Stellenbosch University Animal Care and Use Committee). The animals were eviscerated at abattoirs according to the South African red meat regulations (DAFF (Department of Agriculture Forestry and Fisheries), 2004; Van Schalkwyk & Hoffman, 2010), and transported chilled to the meat laboratory at the Department of Animal Sciences, Stellenbosch University. After 24–48 h post-mortem, the six muscles were removed from the impala and eland carcasses. These were *longissimus thoracis et lumborum* (LTL) located at the 6th rib of the carcasses; *infraspinatus* (IS) and *supraspinatus* (SS) located in the forequarter; and *biceps femoris* (BF), *semitendinosus* (ST) and *semimembranosus* (SM) located in the hindquarter of the carcass. For the ostrich, only five commercially important muscles, (fan fillet (*Muscularis iliotibialis cranialis)*, big drum *(Muscularis femorolibialis medium)*, triangle steak *(Muscularis iliofibularis)*, moon steak *(Muscularis flexor crusis lateralis)* and rump steak *(Muscularis iliotibialis lateralis*), were removed from the leg of the birds. It is important to note that, within the ostrich species there were three genotypes (South African Black, Zimbabwean Blue and Kenyan Red). Identification of the muscles was done by an experienced animal physiologist and verified online (http://bovine.unl.edu/). This information was in turn used to create categories for each muscle type and dummy variables, zero or one, were used to indicated presence or absence during PLS-DA modelling. For example, for category LTL, all LTL muscles would be assigned a one (belonging) and all other muscles a zero (not belonging).

2.2. NIR spectroscopy spectral acquisition

From each carcass, fresh muscles of approximately 2.0–2.5 cm thick steaks were scanned with a portable MicroNIR™ OnSite spectrophotometer (Viavi Solutions®, San Jose, CA, USA) over the NIR range of 908–1700 nm. The illumination source of the spectrophotometer included two joined vacuum tungsten lamps coupled to a linear variable filter and a 128-pixel Indium Gallium Arsenide (InGaAs) photodiode array detector. The InGaAs detector was used to achieve a resolution of 30 μm × 250 μm/50 μm (< 12.5 nm resolution). And, the reflectance spectra were recorded at 6.2 nm intervals, resulting in 125 data points. Each muscle steak was scanned in triplicate at different positions at ambient temperature after allowing a minimum bloom period of 30 min. When scanning, a 2 mm thick glass Steriplan petri dish was placed on top of the meat samples to prevent direct contact of the meat surface moisture with the instrument. Each spectrum was the average of 100 scans, thus a sample spectrum was recorded in about 0.25–0.5 s. An external white and dark reference standards were scanned every 10 min during sample collection. The total number of impala samples scanned were 72 muscles (12 carcasses X 6 different muscles), while the eland's total samples were 90 (15 carcasses X 6 muscles). For ostrich the total number of samples scanned were 75 muscles (15 birds X 5 different muscles).

2.3. Chemical analysis

Moisture, protein and fat content of the game meat steaks were determined as described by Neethling, Hoffman, & Britz, (2014).

2.4. Warner Bratzler shear force (WBSF)

After scanning, the muscle steaks were placed individually into plastic bags that were then submerged into a pre-heated water bath (maintained at 80 °C) for 60 min and then cooled at 4 °C overnight. Once cooled, the samples were then removed from the plastic bags and blotted dry using absorbent paper to remove excess moisture. The cooled cooked meat samples were then used to determine the tenderness using a 3345 model Instron Universal Testing Machine (Apollo Scientific cc, Alberta, Canada) fitted with a Warner-Bratzler blade. Two scalpels fixed at 1 cm from each other were used to cut through the 2 cm thick steaks to produce a rectangular prism of 1 cm × 1 cm × 2 cm that ran parallel with the muscle fibres. Six pieces were removed from each muscle steak and sheared perpendicular to the fibres' longitudinal orientation with a Warner Brazler blade. The average of six measurements was calculated and the value was used to determine the Warner-Bratzler shear force (N) of the muscle, with a greater force being associated with tougher meat (Honikel, 1998).

2.5. Multivariate data analysis

The Unscrambler® X version 10.5 (CAMO Software, Oslo, Norway) and PLS_Toolbox (Version 8.6.2, Eigenvector Research, Inc., Manson, WA USA) data analysis software packages were used to analyse the spectra. The spectral range was reduced from 908–1700 nm to 908–1680 nm to remove the spectral noise segments. As each muscle was scanned three times at different points, spectra were averaged to obtain one spectrum per sample.

2.5.1. Spectral pre-processing

Different pre-processing methods were applied to reduce the scattering effects, baseline shifts and background information (noise) in the data. For impala, ostrich and the combined species, spectra were first treated with standard normal variate (SNV) to remove the scatter effects by centering and scaling each individual spectrum. Detrend transformation was then applied to reduce the baseline shift and curvature in the spectroscopic data (Barnes, Dhanoa, & Lister, 1989). Subsequently, for impala and ostrich, SNV-Detrend was followed by Savitzky-Golay 2nd derivative, 2nd order polynomial, with five smoothing points; while for combined species, 1st derivative was used. Savitzky-Golay 1st and 2nd derivative were applied to smooth the noise fluctuations without introducing distortions to the data, and to expose the peaks that were not clearly visible (Savitzky & Golay, 1964). For the eland muscles, the spectra were only treated with SNV and Savitzky-Golay 2nd derivative, 2nd order polynomial, with five smoothing points.

2.5.2. Principal component analysis

Principal component analysis (PCA), was performed to explore the spectral data and to get an overview of correlations among the muscle types (Cowe & McNicol, 1985; Esbensen, Guyot, Westad, & Houmoller, 2002, pp. 19–74; Wold, 1987). For muscle type discrimination, each species was analysed separately; and then later the different species were collectively analysed regardless of the muscles used.

2.5.3. Calibration and validation (test set) samples

The Kennard-Stone (KS) algorithm was applied to separate the data

Table 2
Proximate chemical composition (moisture, fat and protein) (%) and shear force (WBSF) (N) of impala, eland and ostrich muscles.

Species	Muscle	Moisture (%)	Fat (%)	Protein (%)	WBSF (N)
Impala	LTL	75.5	1.2	22.9	36.9
	BF	75.4	1.6	23.1	44.4
	SM	74.9	1.4	23.5	45.9
	ST	76.1	1.1	22.6	33.6
	IS	76.3	1.9	21.6	28.8
	SS	76.1	1.3	22.1	33.7
Eland	LTL	75.6	1.2	23.0	97.6
	BF	77.8	1.8	20.3	91.5
	SM	76.0	1.6	22.4	78.7
	ST	77.2	1.4	21.3	77.5
	IS	77.3	1.3	21.2	65.5
	SS	77.2	1.6	20.8	89.2
Ostrich	FF	75.6*	1.36*	20.6*	35.8
	RS	76.2*	1.21*	21.4*	56.3
	BD	77.0*	0.95*	20.8*	51.9
	MS	75.8*	1.44*	21.5*	71.0
	TS	77.2*	1.1*	20.7*	46.8
Standard error of laboratory (SEL)	–	0.2	0.27	1.6	8.6

Abbreviations: LTL = *longissimus thoracis et lumborum*, BF = *biceps femoris*, SM = *semimembranosus*, ST = *semitendinosus*, IS = *infraspinatus*, SS = *supraspinatus*, FF = fan fillet, RS = rump steak, BD = big drum, MS = moon steak, TS = triangle steak, WBSF = Warner Bratzler shear force.
*Majewska et al. (2009).

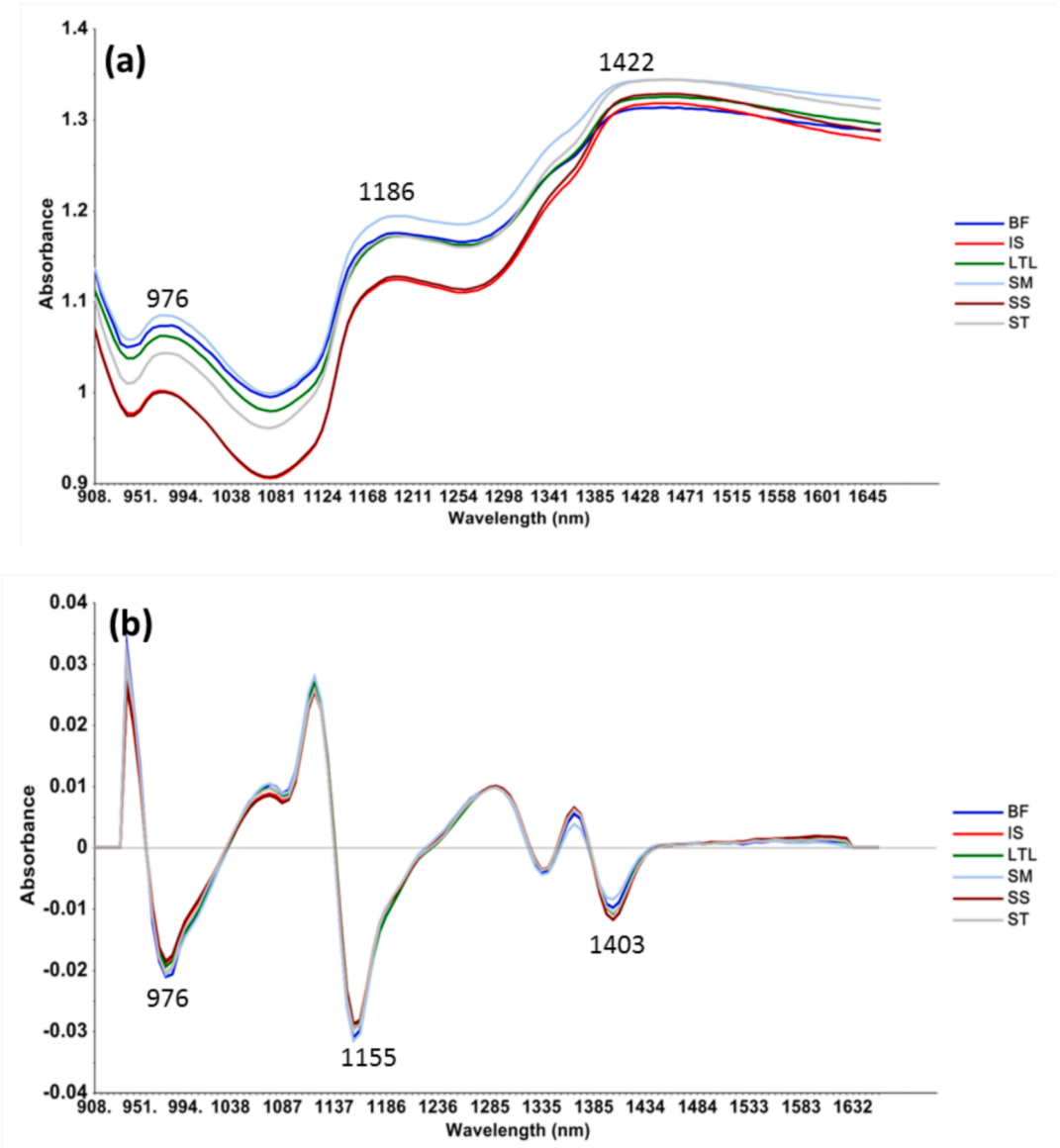

Fig. 1. Mean spectra of impala selected muscles (BF, IS, LTL, SM, SS and ST) showing the wavelength bands of (a) raw spectra, (b) SNV-Detrend and 2nd derivative pre-processed spectra Abbreviations: LTL = *longissimus thoracis et lumborum*, BF = *biceps femoris*, SM = *semimembranosus*, ST = *semitendinosus,* IS = *infraspinatus*, SS = *supraspinatus*.

into a calibration and validation set (Kennard & Stone, 1969). In this approach, a subset of samples providing uniform coverage across the entire data set, including samples on the periphery, are selected. The method begins by finding the two samples which are farthest apart using geometric distance, usually Euclidean distance. To add more samples to the selection set, the algorithm selects from the remaining samples those with the greatest separation distance from the previously selected samples. This process is repeated until the required number of samples, k, have been added to the selection set. In this study, the calibration set was 70% of the original data set and the remaining 30% was used for validation.

2.5.4. Classification

Partial least squares discriminant analysis (PLS-DA) was used to develop models for differentiating the muscle types and species, based on the categories created and the dummy variables assigned, irrespective of muscle used (Barker & Rayens, 2003; Chevallier, Bertrand, Kohler, & Courcoux, 2006; Varmuza & Filzmoser, 2009). Venetian blinds cross-validation was applied to select the optimum number of latent variables (LVs). Subsequently, the models developed were then used to predict unknown samples. When the forequarter, hindquarter and ostrich leg muscles were combined as one class, class modelling was set to “Class Predict Strict”. In the PLS_Toolbox (Version 8.6.2,

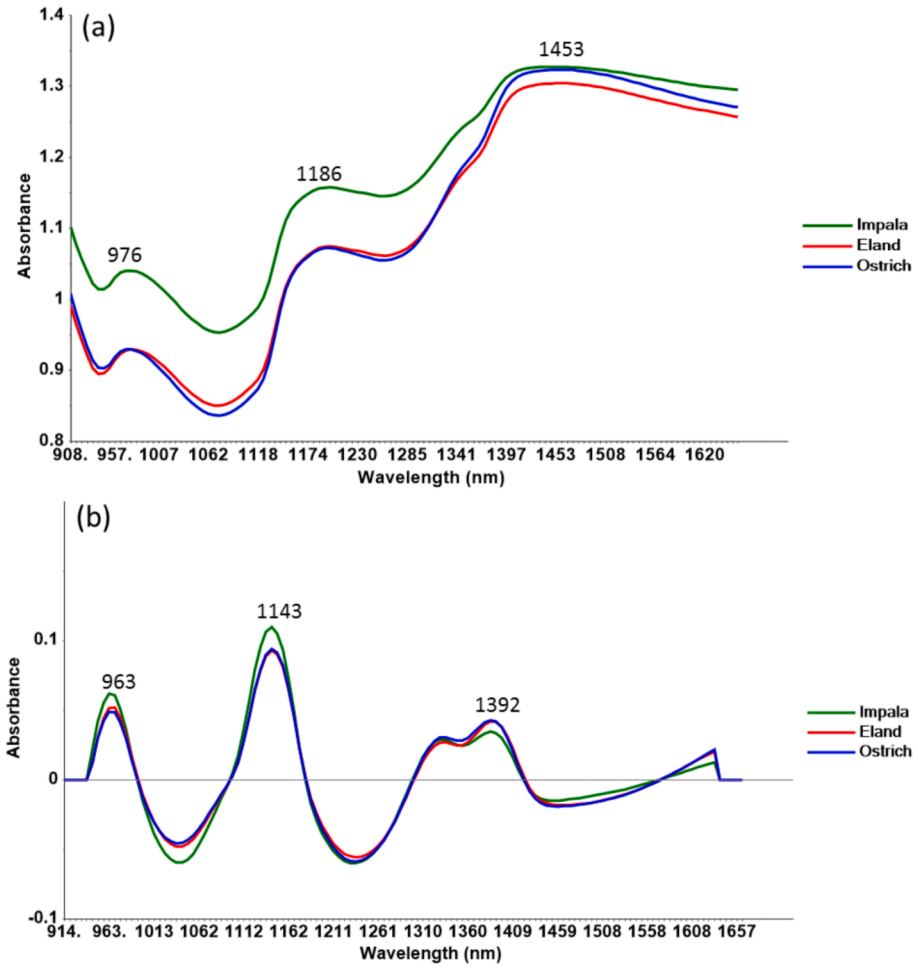

Fig. 2. Mean spectra of impala, eland and ostrich species showing the wavelength bands of (a) raw spectra, (b) SNV-Detrend and 1st derivative pre-processed spectra.

Eigenvector Research, Inc., Manson, WA USA) software, the option "strictthreshold" specifies the "predict strict" classification approach and has a default value of 0.5. This technique reveals only one class that the model is confident to assign each sample. If no class could be assigned to a sample, because the sample's probability is less than the specified threshold, then the sample will be assigned to class zero (0). Afterwards, confusion matrices were used to evaluate the individual models. To interpret the confusion matrix results, percentage classification accuracy was calculated using the following equation (Oliveri & Downey, 2012):

$$\%\ \text{Accuracy} = \frac{TP + TN}{TP + TN + FP + FN} \times 100$$

where:

TP = True positive (samples belonging to the modelled class, if they are correctly predicted to be inside the boundary of that class) e.g. for an LTL class model, true positive samples are LTL samples predicted as such.

FP = False positive (when samples not belonging to the modelled class are incorrectly predicted to be inside the boundary of that class) e.g. in an LTL class model, false positives are samples that are not LTL predicted as LTL.

TN = True negative (samples not belonging to the modelled class, if they are correctly predicted to be outside the boundary of that class) e.g. in an LTL class model, true negatives are samples that are not LTL, predicted as such.

FN = False negative (when samples belonging to the class being modelled are incorrectly predicted to be outside the boundary of that class), e.g. in an LTL class model, false negatives are LTL samples that are misclassified.

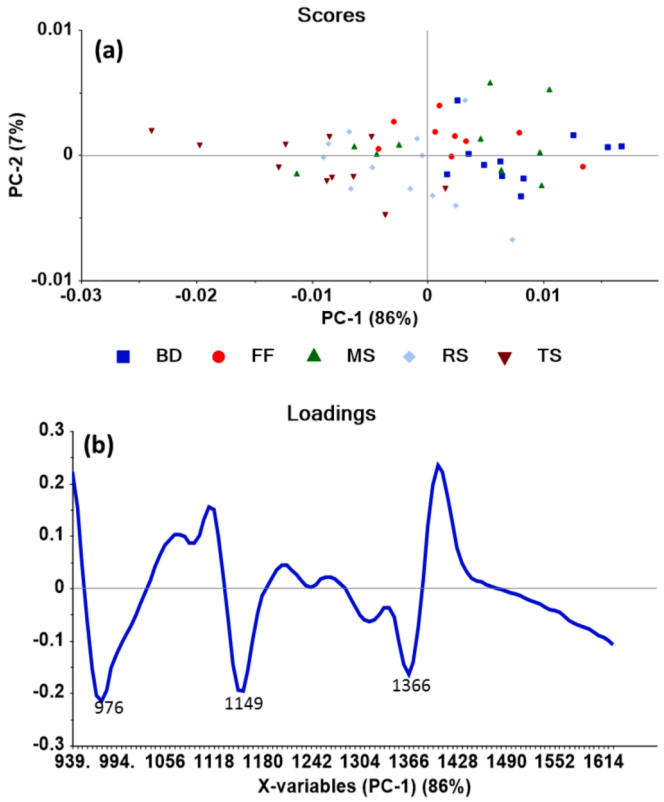

Fig. 3. (a) PCA scores plot of PC1 vs. PC2 contributing 93% explained variance of the model showing the clustering of the ostrich muscle types (SNV-Detrend and 2nd derivative pre-processed spectra). (b) PC1 loadings line plot showing the bands responsible for the clustering of muscle types. Abbreviations: FF = fan fillet, RS = rump steak, BD = big drum, MS = moon steak, TS = triangle steak.

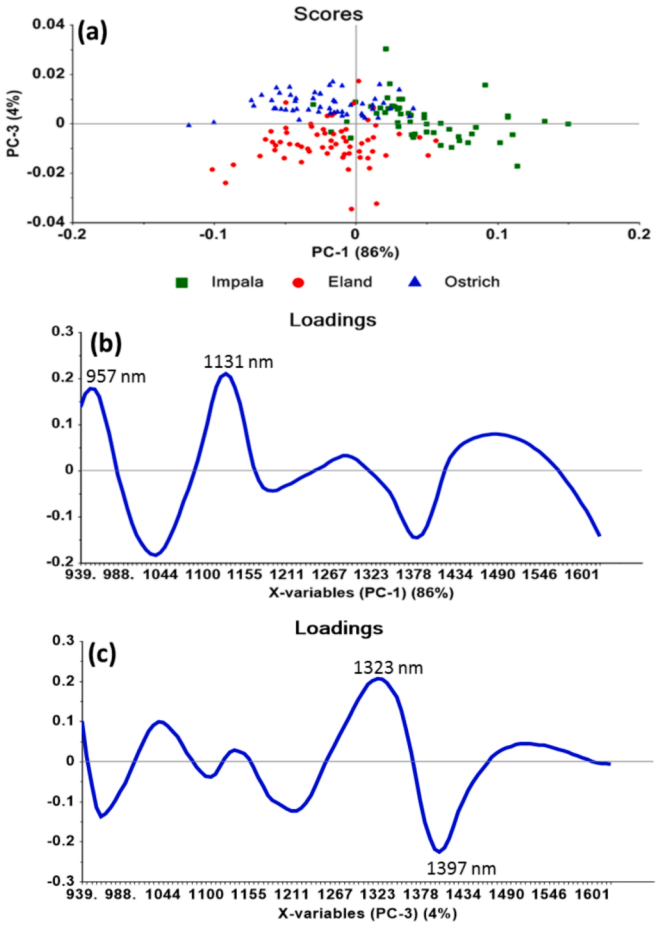

Fig. 4. (a) PCA scores plot of PC1 vs. PC3 contributing 90% of the model showing the clustering of all impala, eland and ostrich muscles irrespective of the type (SNV-Detrend and 1st derivative pre-processed spectra). (b) PC1 and (c) PC3 loadings line plots showing the bands responsible for the clustering of the muscles of these species.

3. Results and discussion

3.1. Physico-chemical analysis

The proximate chemical composition analysis was done to support the spectral interpretation of the species, and the results are presented in Table 2. For the ostrich samples, only the shear force values were analysed from the samples scanned, the proximate analysis values were from a previous study by Majewska et al. (2009) for comparison purposes.

In this study, a moisture content difference of approximately 2% was observed throughout the muscle types of the same species. For impala the moisture ranged from 74.9 to 76.3% where the highest moisture content was obtained from the IS muscle; for eland the moisture ranged from 75.6 to 77.8% where the highest was obtained from the BF muscle. Majewska et al. (2009) reported a moisture difference across the ostrich muscles ranging from 75.6 to 77.2%. In general, the moisture variation of these species between 70 and 77% is supported by Hoffman (2007), even though the eland BF muscle was slightly higher than the other muscles. Likewise, a noticeable protein variation across the muscle types in both impala and eland species was observed. However, there was less variation in fat as compared to other analysis.

It was observed from the eland and impala muscles and also confirmed from the literature (Neethling, Hoffman, & Muller, 2016; Van Heerden, 2018), that the IS muscle is the most tender. Tenderness is a

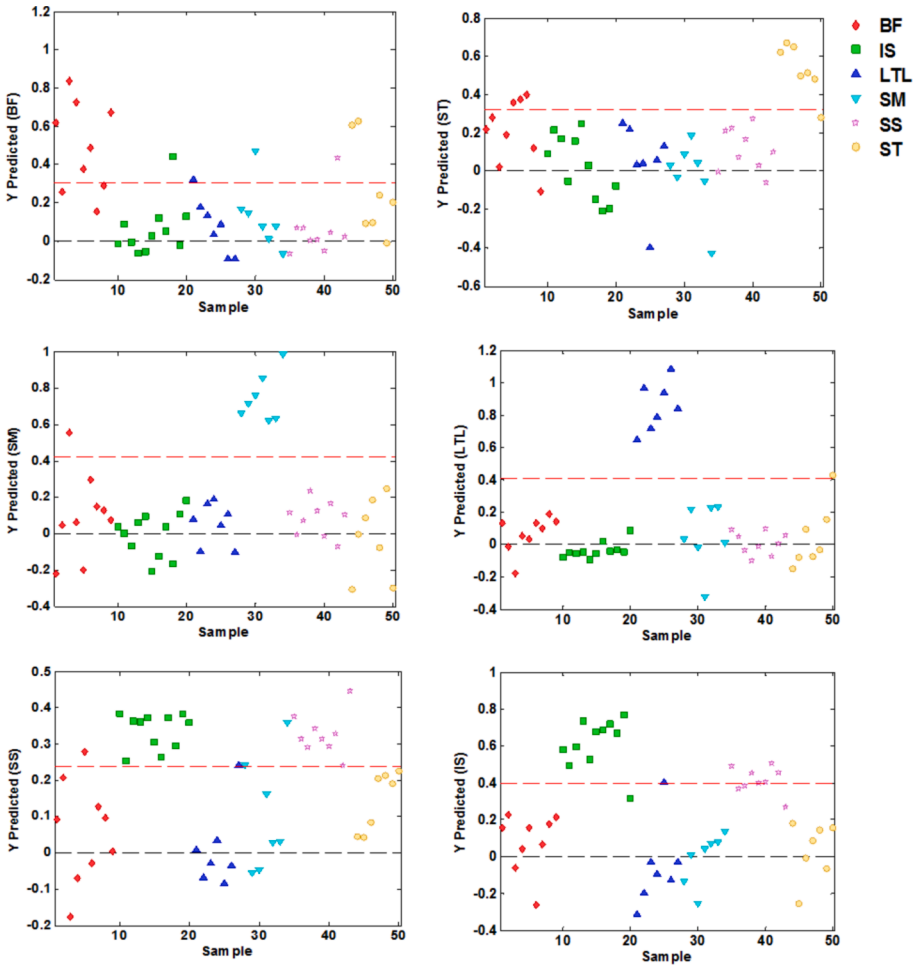

Fig. 5. Score plot obtained by PLS-DA pre-treated with SNV-Detrend and 2nd derivative pre-processing method showing the segregation of impala muscle types. The red dotted line represents the discrimination line. Any sample that is above the red dotted line is regarded as predicted class and any sample that is below the red line is regarded as the other classes not predicted.

Table 3
Confusion matrix obtained with PLS-DA (pre-treated with SNV-Detrend and 2nd derivative) showing muscle types of impala. The true positives, false positives, true negatives, false negatives and the total number of muscle type used for the calibration model are presented.

Class	True + (%)	False + (%)	True - (%)	False - (%)	n
BF	33.0	0.0	100.0	66.7	9
IS	0.0	0.0	100.0	100.0	11
LTL	57.1	2.3	97.7	42.9	7
SM	57.1	0.0	100.0	42.9	7
SS	33.3	2.4	97.6	66.7	9
ST	57.1	2.3	97.7	42.9	7

Abbreviations: LTL = *longissimus thoracis et lumborum*, BF = *biceps femoris*, SM = *semimembranosus*, ST = *semitendinosus,* IS = *infraspinatus*, SS = *supraspinatus*, + = positive, - = negative.

considerable technological parameter used for evaluating the eating quality of meat from a consumer's perception (Cheng, Nicolai, & Sun, 2017). Neethling et al. (2016) reported the SM muscle as the toughest of all, and that was confirmed with the impala muscles (Table 2), with the exception of the eland muscles that showed LTL as the toughest. Regarding the ostrich muscles, FF showed to be the most tender and MS was the toughest.

3.2. Characterisation of NIR spectra

The average NIR spectra of impala selected muscles (BF, IS, LTL, SM, SS and ST) are shown in Fig. 1. The raw spectra (Fig. 1a) of the different muscles adhere to a similar shape even though there are absorbance differences, which could be the associated to differences amongst the muscle types.

In Fig. 1a, two broad absorption bands are observed at 976 and

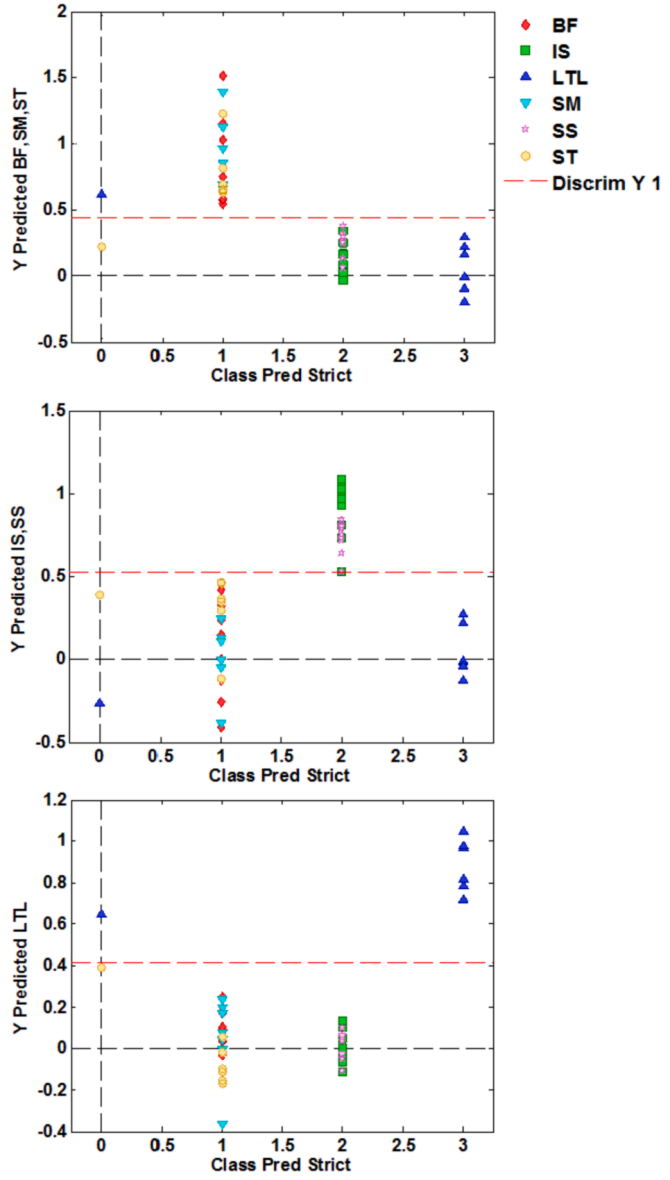

Fig. 6. Class predict strict plot obtained by PLS-DA pre-treated with SNV-Detrend and 2nd derivative pre-processing method showing the segregation of impala muscle types (BF, SM, ST, IS, SS and LTL) when hindquarter muscles are combined as one class, and the forequarter muscles as another. The red dotted line represents the discrimination line. Any sample that is above the red dotted line is regarded as the predicted class and those below the red line are regarded as the other classes not predicted. Samples located at 0 are unassigned samples.
Abbreviations: LTL = *longissimus thoracis et lumborum*, BF = *biceps femoris*, SM = *semimembranosus*, ST = *semitendinosus,* IS = *infraspinatus*, SS = *supraspinatus*.

Table 4
Classification accuracy of PLS-DA models, calibration (Cal) and validation (Val), for discriminating muscles (when hindquarter (BF, SM and ST), forequarter (IS and SS) and ostrich leg (RS and TS) muscles are combined according to their anatomical locations) of impala and ostrich species (SNV-Detrend and 2nd derivative pre-processing) and eland (SNV-2nd derivative pre-processing).

Species	Class	Cal (%)	Val (%)
Impala	BF, SM, ST	97.8	84.6
	IS, SS	100	79.2
	LTL	92.9	100
Eland	BF, SM, ST	85.5	75.9
	IS, SS	92.2	90.4
	LTL	89.1	67.7
Ostrich	BD	95.5	75.0
	MS	88.9	55.3
	FF	85.0	70.0
	RS, TS	87.5	89.7

Abbreviations: LTL = *longissimus thoracis et lumborum*, BF = *biceps femoris*, SM = *semimembranosus*, ST = *semitendinosus,* IS = *infraspinatus*, SS = *supraspinatus*, FF = fan fillet, RS = rump steak, BD = big drum, MS = moon steak, TS = triangle steak.

1422 nm, the bands are related to third and second overtone stretching of the O–H bond (Barbin, Elmasry, Sun, & Allen, 2012; Elmasry, Iqbal, Sun, Allen, & Ward, 2011) that is associated with the water content of the samples. Water is the main component of meat (Table 2). In addition to these, there is a band at 1186 nm that corresponds to the second overtone C–H stretching bond representing the intramuscular fat (Cozzolino & Murray, 2004; Ding & Xu, 2000; Osborne, Fearn, & Hindle, 1993). It is also observed in the raw spectra that IS and SS (forequarter) muscles overlap throughout the wavelength range, while SM and ST (hindquarter) muscles overlap only at 1422 nm. A possible explanation for the overlapping of these muscles might be that they are close in their anatomical location and functions. Neethling, Hoffman, and Britz (2014b) reported similar findings on the effect of season on the chemical composition of male and female blesbok IS and SS muscles. Furthermore, there were noticeable variations between forequarter and hindquarter muscles throughout the spectra. In Fig. 1b (SNV-Detrend, 2nd derivative pre-processed spectra), there are no prominent differences between the muscle types observed at bands located at 976, 1155 and 1403 nm.

The mean spectra of selected muscle types of eland (BF, IS, LTL, SM, SS and ST) and ostrich (BD, MS, FF, RS and TS) are presented in the Appendix, Figs. 1 and 2 respectively. The spectra of eland muscles were very similar to that of impala muscles regarding the shape, absorption bands and the fact that the IS and SS muscles were overlapping. Furthermore, the spectra of ostrich muscles also followed a similar pattern as the impala muscles, except that ostrich had different muscle types. In addition, there was a noticeable difference between the BD and TS muscles. It should be noted that all ostrich muscles are from the leg, unlike other species with muscles from different anatomical locations.

Regarding the mean spectra of impala, eland and ostrich when all muscles were used, Fig. 2 illustrates that there is a visible difference amongst impala and the other two species. Furthermore, some

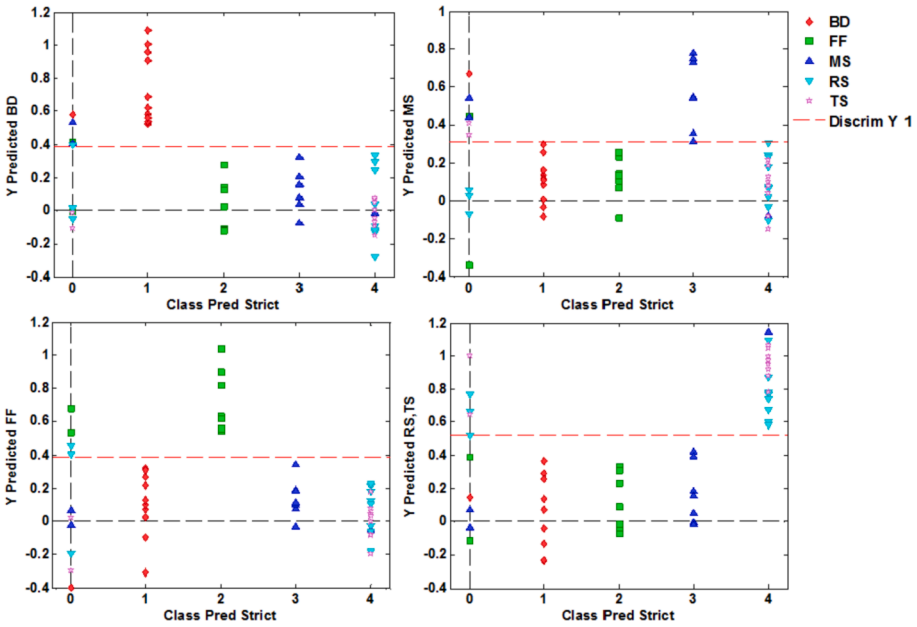

Fig. 7. Class predict strict plot obtained by PLS-DA pre-treated with SNV-Detrend and 2nd derivative pre-processing method showing the segregation of ostrich muscle types (BD, FF, MS, RS and TS) when RS and TS are combined as one class. The red dotted line represents the discrimination line. Any sample that is above the red dotted line is regarded as the predicted class and those below the red line is regarded as the other classes not predicted. Samples located at 0 are unassigned.

overlapping between eland and ostrich at different wavelengths was evident in both the raw (Fig. 2a) and SNV-Detrend and 1st derivative pre-processed spectra (Fig. 2b). The impala muscles had prominent bands situated at 963 and 1143 nm. The 963 nm band is related to the third overtone stretching of an O–H bond (Barbin et al., 2012) associated with the moisture content, and the 1143 nm band corresponds to the second overtone C–H stretching bonds representing the intramuscular fat (Cozzolino & Murray, 2004). Numerous researchers conducting studies on proximate chemical composition of game meat have revealed that the male animals have lower fat and higher moisture contents than females (Von la Chevallerie, 1972; Neethling, Britz, & Hoffman, 2014a; Neethling, Muller, van der Rijst, & Hoffman, 2018). Therefore, the difference in intramuscular fat and moisture content of impala meat compared to the other species might have been caused by the fact that only male impala animals were slaughtered in this study (Table 1). Moreover, the eland and ostrich muscles had an overlapping prominent band situated at 1392 nm, which is associated with the second overtone C–H stretching bond (Cozzolino & Murray, 2004) that is related to the fat content of the samples. Thus, it was easier to observe the differences in spectral features of the different species (Fig. 2b) than to differentiate the spectral features of different muscles within the same species (Fig. 1b).

3.3. Principal component analysis

Fig. 3a shows the PCA scores plot of ostrich muscles (BD, FF, MS, RS and TS) pre-treated with SNV-Detrend and 2nd derivative. The first two principal components (PCs) that explained 93% of the variation, revealed separation only between BD and TS muscles in the direction of PC1. From the PC1 loadings line plot (Fig. 3b), the bands that were most influential for the grouping of these muscles are shown. The wavelength bands at 1149 and 1366 nm represent the C–H bond that corresponds to the fat (Osborne et al., 1993). According to Majewska et al. (2009), BD has the lowest fat content (0.95%) versus TS (1.1%) with higher fat content, which explains the variation between the two muscles. Another band that contributes to the clustering is 976 nm which is related to the third overtone stretching of the O–H bond (Barbin et al., 2012; Elmasry et al., 2011) associated with the moisture content of the samples.

Regarding the impala muscles (BF, IS, LTL, SM, SS and ST), the PCA scores plot of PC1 (73%) versus PC3 (4%), treated with SNV-Detrend and 2nd derivative pre-processing (Appendix, Fig. 3a), showed two clusters separating the muscles. Clustering was according to their anatomical locations. The forequarter (SS and IS) muscles had negative score values, the back (LTL) muscles had positive scores and, the hindquarter (BF, ST and SM) muscles were clustered around the origin; all in the direction of PC3. It was also observed that there was overlapping of SS and IS muscles, which was also noticed in the spectra (Fig. 1a). PC3 loadings line plot (Appendix, Fig. 3b) shows the main wavelength band responsible for the clustering as 1360 nm. This band, the C–H bond, corresponds to the fat (Cozzolino & Murray, 2004). The PCA scores plot and the loadings line plot of eland muscles (Appendix, Fig. 4) follow the same sequence and explanation as impala, except that the clustering is in the direction of PC1.

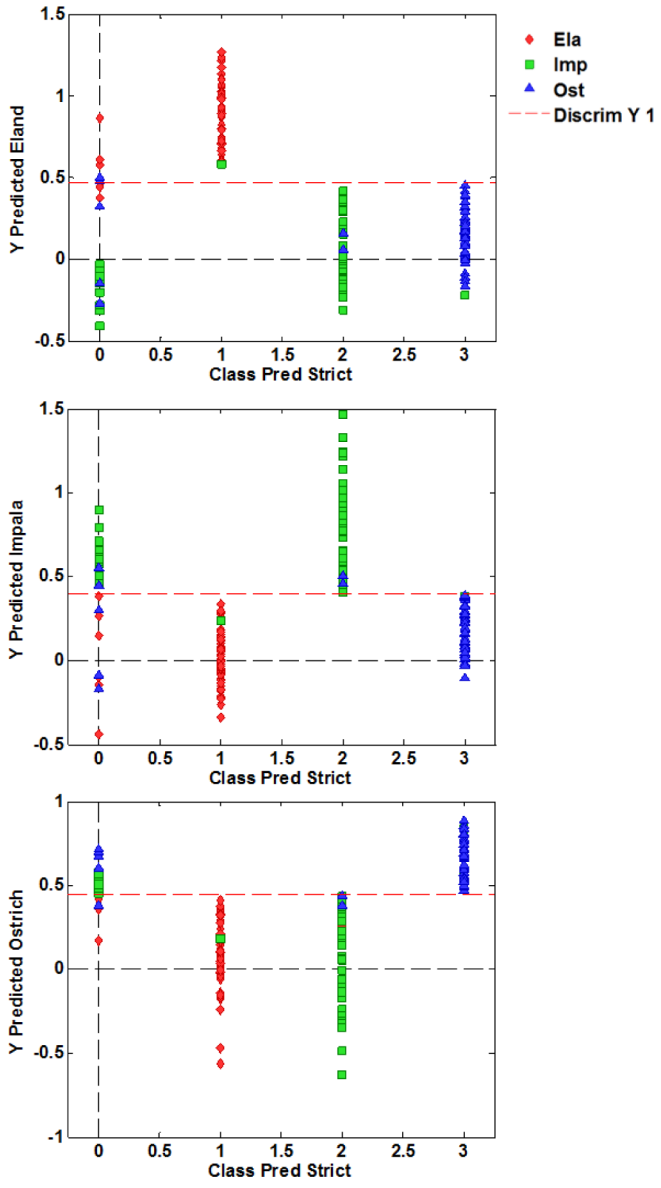

Fig. 8. Class predict strict plot obtained by PLS-DA pre-treated with SNV-Detrend, 1st derivative pre-processing method showing the segregation of all impala, eland and ostrich different muscles. The red dotted line represents the discrimination line. Any sample above the discrimination line is regarded as the predicted class and those below the red line are regarded as the other classes not predicted. Samples located at 0 are unassigned.

Table 5
Percentage accuracy results of PLS-DA models, calibration (Cal) and validation (Val), for classification of all eland, impala and ostrich muscles regardless of the muscle type used (SNV-Detrend and 1st derivative, pre-processing).

Species	Class	PLS-DA	
		Cal (%)	Val (%)
Different species using all muscles	Eland muscles	94	97
	Impala muscles	85	81
	Ostrich muscles	93	92

Table 6
Confusion matrix obtained by PLS-DA showing impala muscle types (pre-treated with SNV-Detrend and 2nd derivative) and different species using all muscles (pre-treated with SNV-detrend and 1st derivative). The true positives, false positives, true negatives, false negatives and the total number of muscles of the models are presented.

Category	Class	True + (%)	False + (%)	True - (%)	False - (%)	n
Impala muscle types	BF, SM, ST	95.7	0.0	100	4.3	23
	IS, SS	100.0	0.0	100	0.0	20
	LTL	85.7	0.0	100	14.3	7
Different species regardless of the muscles	Eland	88.9	1.0	99.0	11.1	63
	Impala	72.0	2.6	97.4	28.0	50
	Ostrich	86.8	1.8	98.2	13.2	53

+ = positive, - = negative.
Abbreviations: LTL = *longissimus thoracis et lumborum*, BF = *biceps femoris*, SM = *semimembranosus*, ST = *semitendinosus*, IS = *infraspinatus*, SS = *supraspinatus*.

Finally, the PCA scores plot presenting all impala, eland and ostrich muscles regardless of the muscle type is shown in Fig. 4. PC1 and PC3 explained 90% of the total variance. Impala samples had positive score values in the direction of PC1, while eland and ostrich had negative and positive score values, respectively, in the direction of PC3. The bands responsible for the clustering of impala muscles are shown in PC1 loadings line plot (Fig. 4b). The main band at 1131 nm represents the C–H bond corresponding to the fat (Osborne et al., 1993), while the 957 nm band represents an O–H bond associated with moisture content. In contrast, PC3 loadings plot (Fig. 4c) shows the major bands contributing to the clustering of the eland and ostrich muscles. The 1323 nm band was responsible for the clustering of ostrich samples, while the 1397 nm band was for the eland samples. Both bands represented the C–H bond associated with the intramuscular fat (Osborne et al., 1993). Additionally, there was some minor overlapping observed between species.

3.4. Classification methods

Fig. 5 shows the PLS-DA scores plot of the impala muscles (BF, IS, LTL, SM, SS and ST), pre-treated with SNV-Detrend and 2nd derivative. Based on cross-validation, five LVs were selected for model calibration with an explained Y variance of 95.6%. For the BF muscle class, six out of nine samples were correctly classified, while two ST and one from each class of LTL, SM, IS and SS muscles were misclassified as BF. For the ST class, six out of seven muscles were correctly classified, whilst three BF (also a hindquarter muscle) samples were misclassified as ST. Misclassification of muscles from the same anatomical location was also observed in the SM class; where one BF muscle was misclassified as SM muscles that were 100% correctly classified. The same misclassification occurred for the forequarter (SS and IS) muscles. However, none was noticed for the LTL class which had a different anatomical location. From the confusion matrix table (Table 3), it is apparent that 100% of the IS muscles were misclassified as SS muscles. This misclassification contributed to the high percentage error of the model that resulted in the 50% classification accuracy for the IS muscles (Table 1, Appendix) of the impala model. The same transpired for the hindquarter (BF, ST and SM) muscles. Misclassification between the hindquarter muscles resulted in a low percentage of correctly predicted (true positive) BF muscles (33%) (Table 3), and low prediction (57.1%) of ST muscles

(Table 1, Appendix). This means the model cannot be used as a reliable tool to authenticate these muscles. Similarly, Sanz et al. (2016) reported difficulty in discriminating multiple muscles (four types) of lamb with hyperspectral imaging. In contrast, Kamruzzaman et al. (2011) managed to discriminate fewer (three) muscle types of lamb meat and obtained 100% classification accuracy. The muscle types that Kamruzzaman et al. (2011) used in their study were also from different anatomical locations. From these results and previous findings from other researchers, it was decided to combine the forequarter (IS and SS) muscles into one class and the hindquarter (BF, ST and SM) muscles into another.

Fig. 6 displays the prediction plot of impala muscle when hindquarter and forequarter muscles were combined. The first four LVs explained 93.9% of the Y variation and was used for model calibration. For the hindquarter muscles, one ST muscle was misclassified as LTL, and one LTL muscle was misclassified as a hindquarter muscle. This is confirmed by the confusion matrix table (Table 6). Furthermore, none of the forequarter muscles were misclassified. The best classification accuracies obtained for these models ranged from 92.9 to 100% (Table 4). These models were validated externally, with samples that were not part of the calibration model and gave excellent results ranging from 79.2 to 100% accuracy. Fig. 5 in the Appendix illustrates the PLS-DA scores plot of eland muscle types pre-treated with SNV-2nd derivative pre-processing. Similar to the impala muscles, the eland model could correctly classify the forequarter, hindquarter and LTL muscles with a classification accuracy rate ranging from 85.5 to 92.2% (Table 4). When assessing the classification accuracies of these two species, it was noted that eland is lower than impala. This could have been caused by the fact that, for this study, there was no variation in sex for impala samples; hence the higher accuracies compared to eland that had almost equal number of sexes (Table 1). This effect of sex needs further investigation.

The PLS-DA scores plot presenting the ostrich muscle types (BD, FF, MS, RS and TS) pre-treated with SNV-Detrend and 2nd derivative technique is shown in Fig. 6 of the Appendix. Based on cross-validation, six LVs were selected for model calibration with an explained Y variance of 98.1%. From the RS muscle class model, it was observed that the majority of TS muscles were misclassified as RS muscles. The misclassification of TS muscles contributed to the lowest percentage of correctly predicted (true positive) TS samples (18.2%) (Table 2, Appendix). Subsequently, that resulted to the lowest classification accuracy (56.7%) of the TS class of the model (Table 1, Appendix). Anatomically, TS and RS muscles are both in the same category of the silver side muscles of the ostrich thigh. It was then decided to classify these muscles as the same category, and the class predict strict plot shown in Fig. 7 is the improved model for ostrich muscles. An explained Y variance of 97.7% described the model calibration selected by six LVs based on cross-validation. In the BD class model, no BD muscles were misclassified. It was observed that only one sample from the MS class was misclassified as the RS/TS class. The same sample from the MS class was detected again in all other class models. In general, no samples were misclassified as other classes, rather they were unassigned (sample either allocated in more than one class or not assigned in any class) with the exception of this MS muscle. Thus, the MS class was the only class with the lowest prediction accuracy (55.3%). The confusion matrix shows no samples were misclassified as BD, FF and MS muscles, however, only 3.3% of other muscles were misclassified as RS/TS (Table 3, Appendix). The classification accuracy obtained for the ostrich model ranged from 85.0 to 95.5% (Table 4). The different ostrich genotypes did not show any visible groupings, hence did not have any influence on the muscle type results. However, the misclassification of the ostrich muscle types might have been caused by the fact that all of these muscles are from the leg, thus similar anatomical locations.

Finally, the three (impala, eland and ostrich) species were discriminated regardless of their muscles and the class predict strict plot pre-treated with SNV-Detrend, 1st derivative pre-processing is shown in Fig. 8. An explained Y variance of 95.3% described the model calibration with five LVs. In all of these class models, there is one similarity; one impala sample was misclassified as eland, one impala was misclassified as ostrich and two ostrich samples were misclassified as impala. As much as there was no class model that attained a 100% classification accuracy, it is however apparent that the models attained good classification accuracies ranging from 85 to 94% (Table 5) with the overall classification accuracies obtained ranging from 70 to 96%. Thus, it has been demonstrated that NIR spectroscopy can discriminate game meat species irrespective of the muscles used. It was expected that there would be a substantial difference when the different muscles were used, since the muscles within each species differ in their anatomical locations and function (Neethling et al., 2016; Van Heerden, 2018).

4. Conclusions

From this study it was confirmed that it is possible to discriminate muscle types of game species with classification accuracies ranging from 85 to 100% using NIR spectroscopy. However, the muscles were discriminated successfully when they were grouped according to their anatomical locations (forequarter, back and hindquarter regions). It was also noted that, muscles that are in the same anatomical location e.g. IS and SS, can be easy targets for fraudsters since it is not easy to distinguish them from one another with NIR spectroscopy. Furthermore, it was easier to classify the different species regardless of the muscle used than to classify the different muscles within the same species. Nevertheless, that was expected as the different species also differ in their DNA. These results reveal the development of classification methods based on NIR analysis for the authentication of impala, eland and ostrich muscles.

Funding

This work is based on the research supported in part by the National Research Foundation (NRF) of South Africa (Unique Grant No. 94031); and South African Research Chairs Initiative (SARChI) funded by the South African Department of Science and Technology (UID: 84633). The authors also wish to acknowledge Pioneer Foods Education and Community Trust, for their financial support providing a student grant for Pholisa Dumalisile.

Ethical approval

All procedures performed in studies involving animals were in accordance with the ethical standards of the institution or practice at which the studies were conducted (approval number: SU-ACUM14-001SOP).

Informed consent

Not applicable.

Declaration of competing interest

Pholisa Dumalisile declares that she has no conflict of interest. Marena Manley declares that she has no conflict of interest. Louwrens Hoffman declares that he has no conflict of interest. Paul J. Williams declares that he has no conflict of interest.

Acknowledgements

This work is based on the research supported in part by the National Research Foundation (NRF) of South Africa (Unique Grant No. 94031); and South African Research Chairs Initiative (SARChI) funded by the South African Department of Science and Technology (UID: 84633). The authors also wish to acknowledge Pioneer Foods Education and Community Trust, for their financial support providing a student grant for Pholisa Dumalisile.

Opinions expressed, and conclusions arrived at, are those of the authors and are not necessarily to be attributed to the NRF.

Appendix

Tables 1–3 and Figs. 1–6 are given in this appendix. The large amount of data generated was placed in a separate appendix to simplify the discussion section of this paper.

Abbreviations: LTL = *longissimus thoracis et lumborum*, BF = *biceps femoris*, SM = *semimembranosus*, ST = *semitendinosus,* IS = *infraspinatus*, SS = *supraspinatus*, FF = fan fillet, RS = rump steak, BD = big drum, MS = moon steak, TS = triangle steak, + = positive, - = negative.

Table 1
Percentage accuracies of PLS-DA models showing calibration (Cal) and validation (Val), for the classification of different muscles of impala and ostrich species pre-treated with SNV-Detrend and 2nd derivative pre-processing

Species	Muscle	Cal (%)	Val (%)
Impala	BF	66.7	66.7
	IS	50.0	50.0
	LTL	77.4	90.0
	SM	78.6	70.0
	SS	65.4	64.0
	ST	77.4	57.1
Ostrich	BD	90.9	62.5
	FF	82.2	58.4
	MS	85.0	70.0
	RS	73.8	100
	TS	56.7	50.0

Table 2
Confusion matrix obtained with PLS-DA (pre-treated with SNV-Detrend and 2nd derivative) showing muscle types of ostrich The true positives, false positives, true negatives, false negatives and the total number of muscle type used for the calibration model are presented.

Class	True + (%)	False + (%)	True - (%)	False - (%)	n
BD	81.8	0.0	100	18.2	11
FF	66.7	2.3	97.7	33.3	9
MS	70.0	0.0	100	30.0	10
RS	50.0	2.4	97.6	50.0	12
TS	18.2	4.8	95.2	81.8	11

Table 3
Confusion matrix obtained with PLS-DA showing muscle types (when certain muscles are combined according to their anatomical locations) of eland (pre-treated with SNV-2nd derivative) and ostrich (pre-treated with SNV-Detrend and 2nd derivative). The true positives, false positives, true negatives, false negatives and the total number of muscle type used for the calibration model are presented.

Species	Class	True + (%)	False + (%)	True - (%)	False - (%)	N
Eland	BF,SM,ST	80.0	9.1	90.1	20.0	30
	IS,SS	87.0	2.5	97.5	13.0	23
	LTL	80.0	1.9	98.1	20.0	10
Ostrich	BD	90.9	0.0	100	9.1	11
	FF	77.8	0.0	100	22.2	9
	MS	70.0	0.0	100	30.0	10
	RS,TS	78.3	3.3	96.7	21.7	23

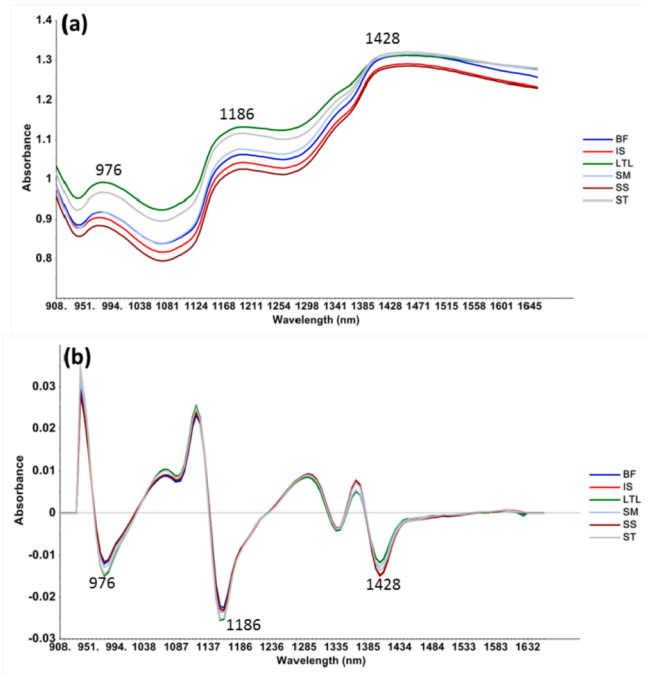

Fig. 1. Mean spectra of eland muscles (BF, IS, LTL, SM, SS and ST) showing the wavelength bands of (a) raw spectra, (b) SNV-2nd derivative pre-processed spectra.

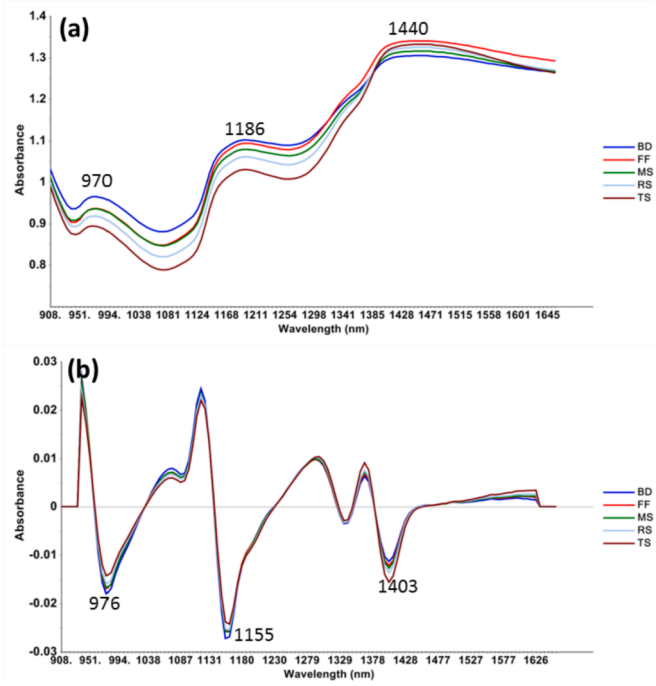

Fig. 2. Mean spectra of ostrich muscles (BD, MS, FF, RS and TS) showing the wavelength bands of (a) raw spectra, (b) SNV-Detrend and 2nd derivative pre-processed spectra.

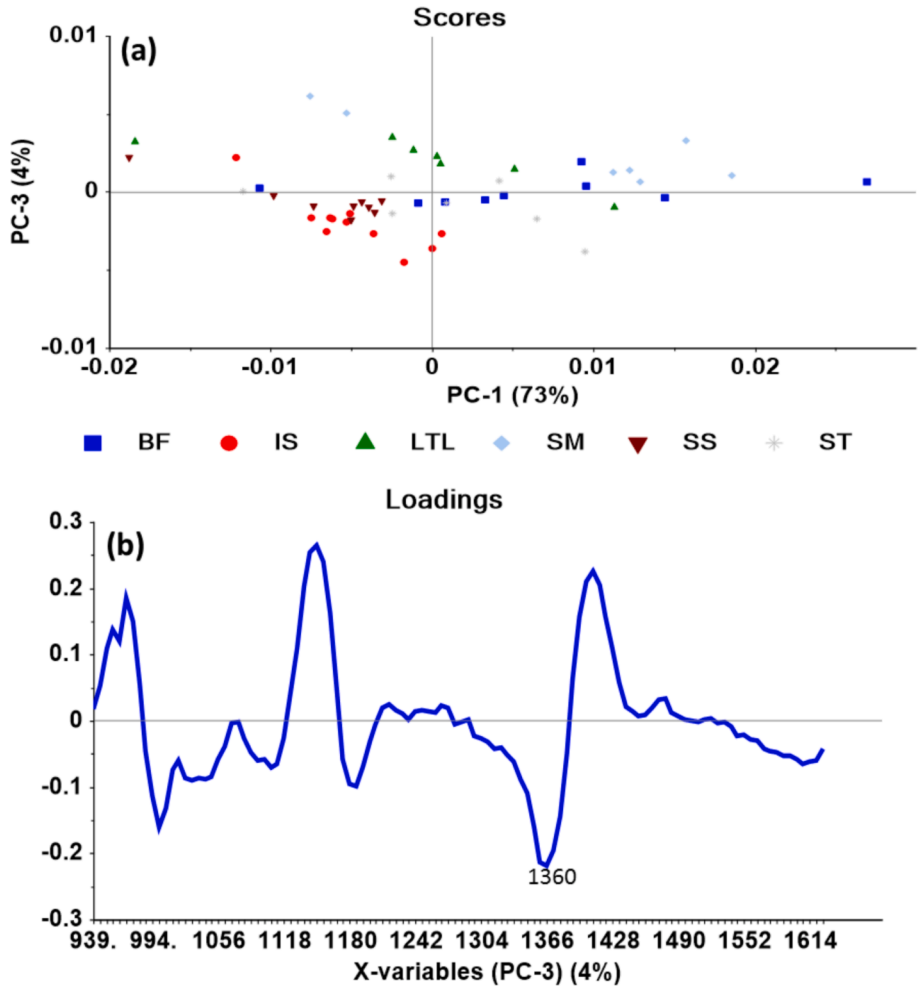

Fig. 3. (a) PCA scores plot of PC1 vs. PC3 accounting 77% explained variation of the model showing the clustering of the impala muscle types (SNV-Detrend and 2nd derivative pre-processed spectra). (b) PC3 loadings line plot showing the band responsible for the groupings of the muscle types.

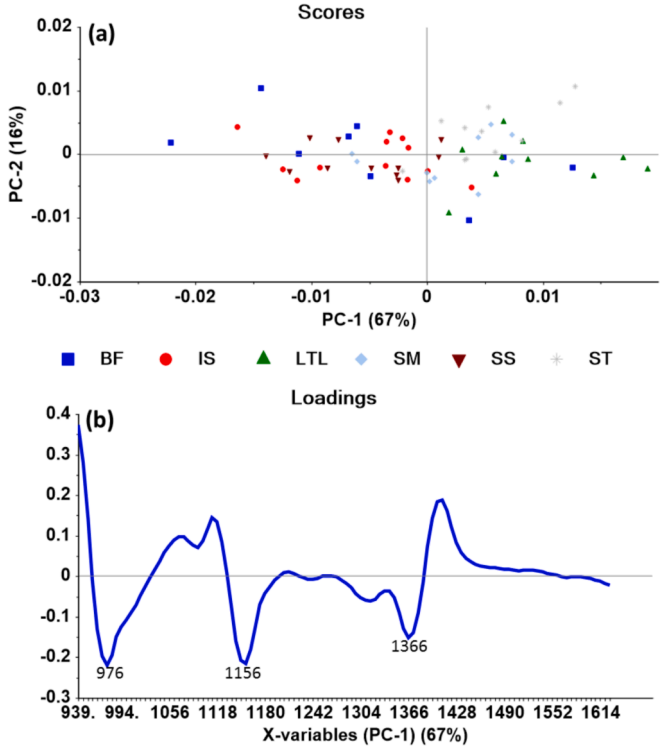

Fig. 4. (a) PCA scores plot of PC1 vs. PC2 contributing 83% explained variance of the model showing the clustering of the eland muscle types (SNV-2nd derivative pre-processed spectra). (b) PC1 loadings line plot showing the bands responsible for the clustering of muscle types.

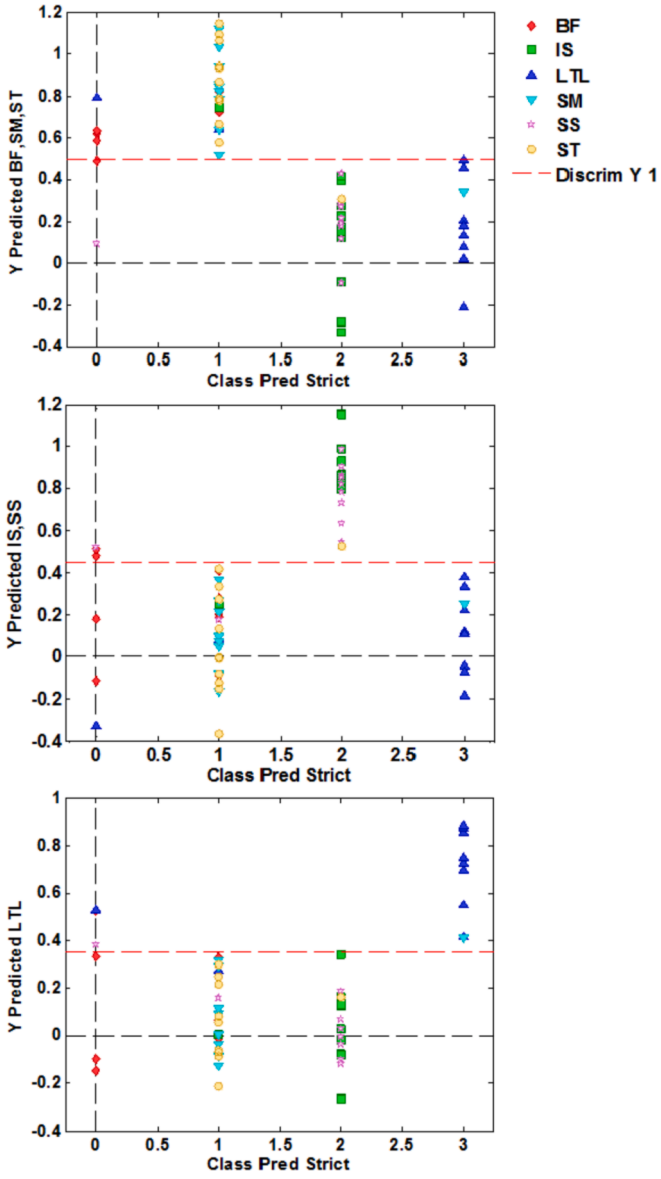

Fig. 5. Class predict strict plot obtained by PLS-DA pre-treated with SNV-2nd derivative pre-processing method showing the segregation of eland muscle types. The red dotted line represents the discrimination line. Any sample that is above the red dotted line is regarded as predicted in that class and those below the red line are regarded as the other classes not predicted in this class. Samples located at 0 are unassigned samples.

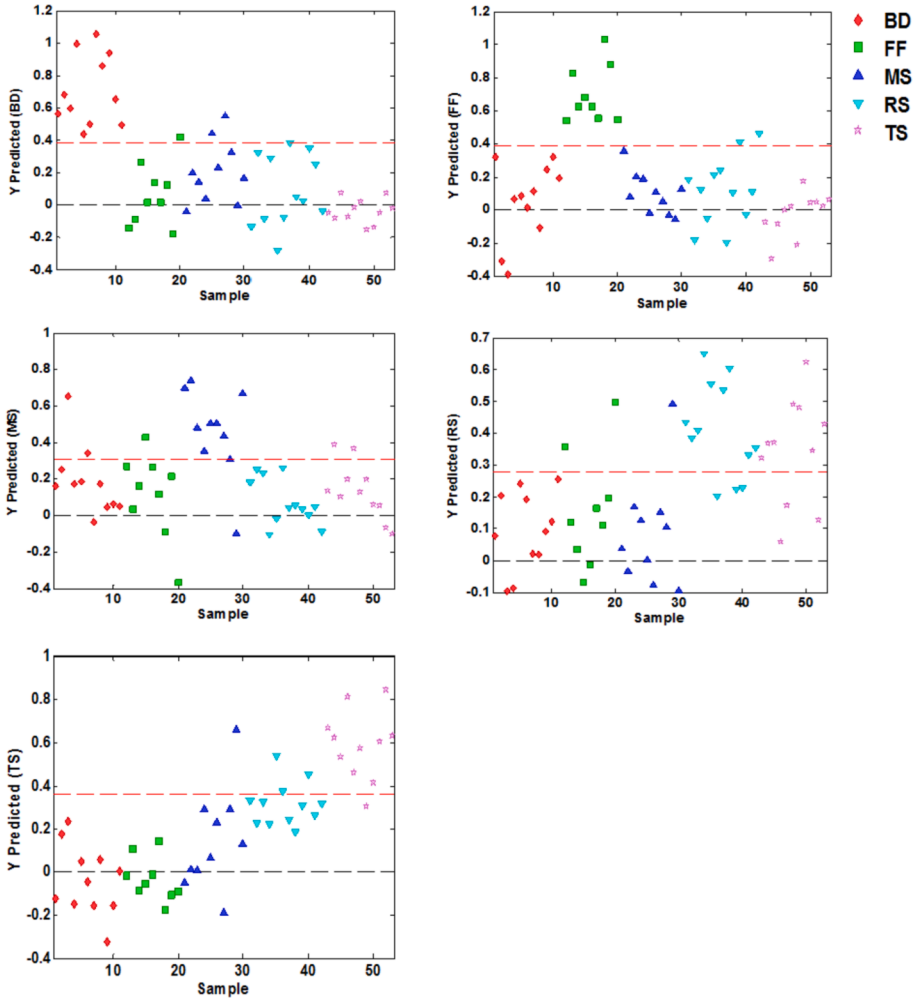

Fig. 6. Scores plot obtained by PLS-DA pre-treated with SNV-Detrend and 2nd derivative pre-processing method showing the segregation of ostrich muscle types. The red dotted line represents the discrimination line. Any sample that is above the red dotted line is regarded as predicted class and any sample that is below the red line is regarded as the other classes not predicted.

References

Alomar, D., Gallo, C., Castañeda, M., & Fuchslocher, R. (2003). Chemical and discriminant analysis of bovine meat by near infrared reflectance spectroscopy (NIRS). *Meat Science, 63*(4), 441–450.

Barbin, D., Elmasry, G., Sun, D. W., & Allen, P. (2012). Near-infrared hyperspectral imaging for grading and classification of pork. *Meat Science, 90*(1), 259–268.

Barker, M., & Rayens, W. (2003). Partial least squares for discrimination. *Journal of Chemometrics, 17*(3), 166–173.

Barnes, R. J., Dhanoa, M. S., & Lister, S. J. (1989). Standard normal variate transformation and de-trending of near-infrared diffuse reflectance spectra. *Applied Spectroscopy, 43*, 772–777.

Cawthorn, D. M., Steinman, H. A., & Hoffman, L. C. (2013). A high incidence of species substitution and mislabelling detected in meat products sold in South Africa. *Food Control, 32*(2), 440–449.

Cheng, J. H., Nicolai, B., & Sun, D. W. (2017). Hyperspectral imaging with multivariate analysis for technological parameters prediction and classification of muscle foods: A review. *Meat Science, 123*, 182–191.

Chevallier, S., Bertrand, D., Kohler, A., & Courcoux, P. (2006). Application of PLS-DA in multivariate image analysis. *Journal of Chemometrics, 20*, 221–229.

Cowe, A., & McNicol, J. W. (1985). The use of principal components in the analysis of near infrared spectra. *Applied Spectroscopy, 39*(2), 257–266.

Cozzolino, D., & Murray, I. (2004). Identification of animal meat muscles by visible and near infrared reflectance spectroscopy. *Lebensmittel-Wissenschaft und -Technologie-Food Science and Technology, 37*(4), 447–452.

DAFF (Department of Agriculture, Forestry and Fisheries). (2004). *Meat safety Act (Act No. 40 of 2000), red meat regulations (No. R. 1072 of 17 september 2004) (regulation gazette No. 8056).* South Africa: Government Printing Offices.

Danezis, G. P., Tsagkaris, A. S., Camin, F., Brusic, V., & Georgiou, C. A. (2016). Food authentication: Techniques, trends & emerging approaches. *TRAC Trends in Analytical Chemistry, 85*, 123–132.

Ding, H. B., & Xu, R. J. (2000). Near-infrared spectroscopic technique for detection of beef hamburger adulteration. *Journal of Agricultural and Food Chemistry, 48*(6), 2193–2198.

DoA (Department of Agriculture) (2015). *Agricultural product standards Act, 1990 (Act 119 of 1990): Regulations regarding the classification and marking of meat intended for sale in the republic of South Africa (R. 55/2015).* South Africa: Government Printing Offices.

DoH (Department of Health) (2014). *Foodstuffs, Cosmetics and disinfectants Act, 1972 (Act 54 of 1972): Regulations relating to the labelling and advertising of foods: Amendment (R. 429/2014).* South Africa: Government Printing Offices.

Elmasry, G., Iqbal, A., Sun, D. W., Allen, P., & Ward, P. (2011). Quality classification of cooked, sliced Turkey hams using NIR hyperspectral imaging system. *Journal of Food Engineering, 103*(3), 333–344.

Esbensen, K. H., Guyot, D., Westad, F., & Houmoller, L. P. (2002). *Principal Component Analysis (PCA) - introduction Multivariate data analysis - in practice: An introduction to multivariate data analysis and experimental design.* Camo ASA19–74.

Fajardo, V., González Isabel, I., Rojas, M., García, T., & Martín, R. (2010). A review of current PCR-based methodologies for the authentication of meats from game animal species. *Trends in Food Science & Technology, 21*(8), 408–421.

Fisher, R. A. (1936). The use of multiple measurements in taxonomic problems. *Annals of Eugenics, 7*, 179–188.

Hoffman, L. C. (2007). *The meat we eat: Are you game? Inaugural addess.* Western Cape, South Africa: Stellenbosch University.

Honikel, K. O. (1998). Reference methods for the assessment of physical characteristics of meat. *Meat Science, 49*(4), 447–457.

Jonker, K. M., Tilburg, J. J. H. C., Hagele, G. H., & de Boer, E. (2008). Species identification in meat products using real-time PCR. *Food Additives & Contaminants. Part A, Chemistry, Analysis, Control, Exposure & Risk Assessment, 25*(5), 527–533.

Kamruzzaman, M., Elmasry, G., Sun, D. W., & Allen, P. (2011). Application of NIR hyperspectral imaging for discrimination of lamb muscles. *Journal of Food Engineering, 104*(3), 332–340.

Kamruzzaman, M., Sun, D. W., ElMasry, G., & Allen, P. (2013). Fast detection and visualization of minced lamb meat adulteration using NIR hyperspectral imaging and multivariate image analysis. *Talanta, 103*, 130–136.
Kennard, R. W., & Stone, L. A. (1969). Computer aided design of experiments. *TechnoMetrics, 11*(1), 137–148.
Majewska, D., Jakubowska, M., Ligocki, M., Tarasewicz, Z., Szczerbińska, D., Karamucki, T., et al. (2009). Physicochemical characteristics, proximate analysis and mineral composition of ostrich meat as influenced by muscle. *Food Chemistry, 117*(2), 207–211.
Manley, M. (2014). Near-infrared spectroscopy and hyperspectral imaging: Non-destructive analysis of biological materials. *Chemical Society Reviews, 43*(24), 8200–8214.
Nakyinsige, K., Man, Y. B. C., & Sazili, A. Q. (2012). Halal authenticity issues in meat and meat products. *Meat Science, 91*(3), 207–214.
Neethling, J., Britz, T. J., & Hoffman, L. C. (2014a). Impact of season on the fatty acid profiles of male and female blesbok (Damaliscus pygargus phillipsi) muscles. *Meat Science, 98*(4), 599–606.
Neethling, J., Hoffman, L. C., & Britz, T. J. (2014b). Impact of season on the chemical composition of male and female blesbok (*Damaliscus pygargus phillipsi*) muscles. *Journal of the Science of Food and Agriculture, 94*(3), 424–431.
Neethling, J., Hoffman, L. C., & Muller, M. (2016). Factors influencing the flavour of game meat: A review. *Meat Science, 113*(November), 139–153.
Neethling, J., Muller, M., van der Rijst, M., & Hoffman, L. C. (2018). Sensory quality and fatty acid content of springbok (Antidorcas marsupialis) meat: Influence of farm location and sex. *Journal of the Science of Food and Agriculture, 98*(7), 2548–2556.
Oliveri, P., & Downey, G. (2012). Multivariate class modeling for the verification of food-authenticity claims. *TRAC Trends in Analytical Chemistry, 35*, 74–86.
Osborne, B. G., Fearn, T., & Hindle, P. H. (1993). *Practical NIR spectroscopy with applications in food and beverage analysis* (2nd ed.). Essex: Longman Scientific & Technical.
O'Mahony, P. J. (2013). Finding horse meat in beef products-a global problem. *QJM, 106*(6), 595–597.
Sanz, J. A., Fernandes, A. M., Barrenechea, E., Silva, S., Santos, V., Gonçalves, N., et al. (2016). Lamb muscle discrimination using hyperspectral imaging: Comparison of various machine learning algorithms. *Journal of Food Engineering, 174*, 92–100.
Savitzky, A., & Golay, M. J. E. (1964). Smoothing and differentiation of data by simplified least squares procedures. *Analytical Chemistry, 36*(8), 1627–1639.
Soon, J. M., & Manning, L. (2018). Food smuggling and trafficking: The key factors of influence. *Trends in Food Science & Technology, 81*(May), 132–138.
Spink, J., & Moyer, D. C. (2011). Defining the public Health threat of food fraud. *Journal of Food Science, 76*(9), 157–163.
Van Ba, H., Park, K., Dashmaa, D., & Hwang, I. (2014). Effect of muscle type and vacuum chiller ageing period on the chemical compositions, meat quality, sensory attributes and volatile compounds of Korean native cattle beef. *Animal Science Journal, 85*(2), 164–173.
Van Heerden, A. M. (2018). *Profiling the meat quality of blue wildebeest (Connochaetes taurinus), Dissertation presented for the degree of Master of Science (Animal Science)* Stellenbosch: Stellenbosch University.
Van Ruth, S. M., Luning, P. A., Silvis, I. C. J., Yang, Y., & Huisman, W. (2018). Differences in fraud vulnerability in various food supply chains and their tiers. *Food Control, 84*, 375–381.
Van Schalkwyk, D. L., & Hoffman, L. C. (2010). *Guidelines for the harvesting of game for meat export.* Windhoek, Namibia: Printech cc 71pp.
Varmuza, K., & Filzmoser, P. (2009). Chemoinformatics-chemometrics-statistics. *Introduction to multivariate statistical analysis in chemometrics* (pp. 1–26). Boca Raton, FL: CRC Press Taylor and Francis Group.
Verbeke, J., & Ward, R. W. (2006). Consumer interest in information cues denoting quality, traceability and origin: An application of ordered probit models to beef labels. *Food Quality and Preference, 17*, 453–467.
Von la Chevallerie, M. (1972). Meat quality of seven wild ungulate species. *South African Journal of Animal Science, 2*, 101–103.
Walker, M. J., Burns, M., & Burns, D. T. (2013). Horse meat in beef products- species substitution 2013. *Journal of the Association of Public Analysts, 41*, 67–106.
Wold, S. (1987). Principal component analysis. *Chemometrics and Intelligent Laboratory Systems, 2*, 37–52.